First publ. in: Berichte der Bunsen-Gesellschaft 98 (1994), 3, pp. 461-465

Phase Transitions at Quantum Surfaces

P. Leiderer

Fakultät für Physik, Universität Konstanz, D-78434 Konstanz, Germany

Key Words: Adsorption / Critical Phenomena / Interfaces / Phase Transitions / Surfaces

The quantum systems helium and hydrogen provide a versatile testing ground for studying interfacial phenomena. As examples, both some properties of surfaces near thermodynamic equilibrium, like layering and wetting, and nonequilibrium states of quench-condensed disordered films are discussed. A further topic is the development of macroscopic instabilities of interfaces under external perturbation.

I. Introduction

Surface phenomena of condensed quantum matter, mostly helium and hydrogen, have raised considerable interest in recent years for a number of reasons. Although not very important for direct applications, these systems display several properties which make them ideal candidates for fundamental studies. Since the interactions between the simple atoms and molecules under consideration are accessible from ab initio calculations, good quantitative comparisons between theory and experiments should be possible. Furthermore the systems can be prepared in general under extremely pure and well-defined conditions. As a result of the small mass and low interaction energies, effects due to zero point motion should be particularly prominent in these quantum liquids and solids. The superfluid transitions in ^{3}He and ^{4}He, resulting from quantum statistics, add to the intriguing properties of these systems, and there are various novel interfacial phenomena, like melting-crystallization waves, which for various reasons have so far only been observed in quantum systems.

Thin films of helium and hydrogen with a thickness in the monolayer range have been studied quite thoroughly, both regarding structure and excitations, by means of neutron scattering, specific heat, third sound etc., in particular on substrates with large surface area like exfoliated graphite, as described in several review articles [1]. Here we focus on investigations of films with a thickness beyond 1 monolayer, concentrating on phenomena like layering and wetting, and the annealing of disordered films. At the end we shall also consider the stability of the surfaces of the bulk solid and liquid phases with respect to external perturbations, like electrostatic pressure, and illustrate the formation of surface patterns developing as the system is driven beyond the stability threshold. Due to space limitations only part of the work done on these topics can be presented here, and the selection is certainly biased, most of the examples being taken from our own investigations. Important subjects, in particular the roughening transitions of solid-liquid He interfaces, which are not treated here, have been reviewed elsewhere in the literature [2]. The wetting behavior of He on alkali metals, another question which has raised a large amount of interest recently, is discussed in this volume by Taborek [3].

II. Quantum Films Close to Equilibrium

In this section we discuss some structural and dynamic properties of helium and hydrogen surfaces close to thermodynamic equilibrium. In many respects the two materials are qualitatively similar; others, like superfluidity and the absence of a conventional triple point for helium, are a manifestation of the more pronounced quantum nature of the helium systems.

a) Helium

Bulk helium, due to its large zero point motion, does not solidify unless sufficient pressure – 25 bar in the case of ^{4}He below 1 K – is applied. A thin film of ^{4}He on a strong binding material such as graphite, however, is subject to large van der Waals forces exerted by the substrate, and as a result the first two monolayers have a crystalline structure. Since the van der Waals pressure drops rapidly with increasing distance, the lattice constant of the second layer is somewhat larger than for the first layer, as demonstrated, e.g., by means of neutron diffraction [4]. The third and higher monolayers do not display Bragg peaks, thus indicating a fluid phase. The characteristic excitations of bulk superfluid ^{4}He, phonons and rotons, only start to show up at the beginning of the fourth layer.

In the case of superfluid ^{4}He it was also possible to detect elementary excitations at the liquid surface – so-called ripplons – on an Ångstrom scale [5], whereas usually ripplons are overdamped at such small wavelengths. The ripplon spectrum evolves from the dispersion relation of classical capillary waves, but deviates significantly at large wave vectors around 1 $Å^{-1}$ due to the atomic structure of the liquid.

Another phenomenon which has been demonstrated most clearly for He films is the formation of a layerlike structure in the liquid close to a solid wall. Layering has shown up in various experimental quantities like adsorption isotherms, third sound, specific heat and, in a very pronounced way, in the mobility of surface state electrons. As an example, mobility results are shown in Fig. 1 for a liquid ^{4}He film growing on crystalline H_2 [6]: The surface state electrons, which are used as a probe here, are located outside the liquid slightly above the surface (some 100 or 20 Å in the

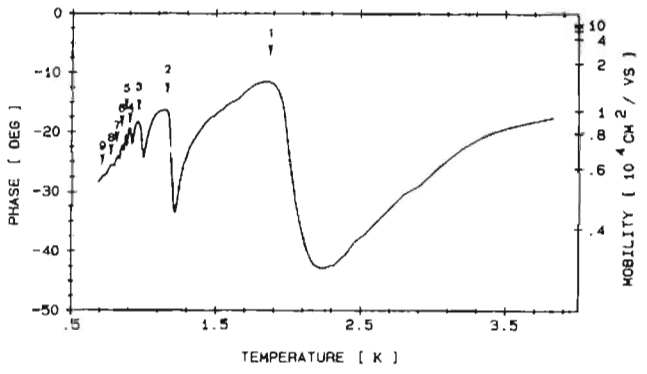

Fig. 1
Electron mobility on solid hydrogen covered with a ^{4}He film whose thickness increases as the temperature is lowered. The figures indicate the number of monolayers completed at the respective temperatures (after Ref. 6)

case of helium and hydrogen, respectively) and are very sensitive to density fluctuations at the surface, because these act as scattering centres and hence decrease the electron mobility. As the first monolayer of He starts to build up on the H_2 substrate, the mobility first drops, but then rises again, reaching nearly the starting value (on the bare H_2 substrate) at monolayer completion. This shows that the full first He layer is as smooth as the substrate. An analogous behavior is observed for the second and, in a less and less pronounced way, for the subsequent layers. In total 9 oscillations in the mobility can be resolved in Fig. 1, layering hence extends surprisingly far into the bulk liquid.

An analysis of the data in Fig. 1 for the second and higher layers yields, as a by-product, the van der Waals coefficient for ^{4}He on H_2. The resulting value, 20 K (layer)^3, is distinctly larger (by about a factor of two) than theoretical estimates [7]. This discrepancy is puzzling, because, as mentioned in the introduction, interaction potentials between He and H_2 are well-known. Since the same experimental value has been found in several independent measurements using different techniques [8–10], the discrepancy is unlikely to be attributable to an experimental artefact, and therefore deserves further attention.

The substrate-adsorbate combination of H_2 and ^{4}He is interesting also for another reason: due to the weak binding – the binding energy as determined from Fig. 1 amounts to somewhat less than 10 K – the first helium layer should be just at the borderline between being liquid and solid [11]. An experiment with surface state electrons [12] did not give any hint for solidification up to monolayer completion; at slightly higher coverage, however, an anomaly in the electron mobility was observed, as shown in Fig. 2, which suggests that the first helium layer in fact solidifies under the additional pressure of the beginning second layer.

b) Hydrogen

A central aspect of physisorbed films is the question whether complete or incomplete wetting occurs, i.e. whether in thermodynamic equilibrium the film thickness diverges or remains finite when the system approaches the saturated vapor pressure. The actual behavior is determined by a subtle balance between the interaction among the adsorbate molecules and the adsorbate-substrate interaction. The degree of wetting in general also depends on temperature, which can lead to a phase transition from incomplete to complete wetting. For simple systems this transition is frequently found to take place at the triple point, a behavior which, as shown below, also holds for hydrogen on noble metal substrates [13, 14].

As an example, we have plotted in Fig. 3a the thickness of a saturated H_2 film on gold as a function of temperature. The film thickness d was measured in this case by means of surface plasmon resonance [13] in a closed cell at a height of 1 cm above the coexisting bulk hydrogen sample. When the temperature was changed, d relaxed towards its new equilibrium value d_s within a time shorter than the time constant of the electronics, about 5 s. Starting below the triple temperature T_3 and increasing T leads to a growth of the film thickness, whereas above T_3 the value of d stays essentially constant. Near T_3 a discontinuous jump from the low to the high temperature branch (or vice versa, if T is decreasing) is observed, which depends in its details on the rate of the temperature change.

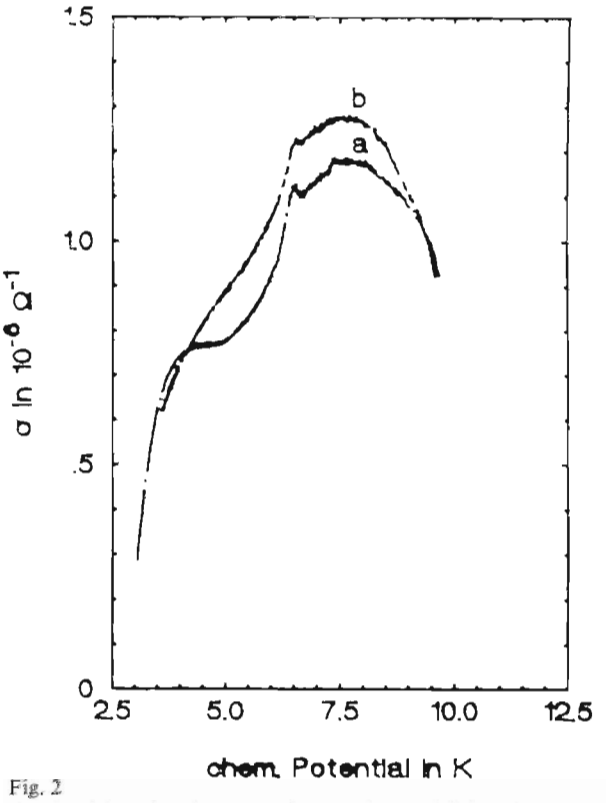

Fig. 2
Conductivity of surface state electrons in the vicinity of the completion of the first ^{4}He monolayer on solid hydrogen, plotted vs. the chemical potential $\Delta\mu/k_B = T \ln(p_s/p)$, where p_s is the (temperature dependent) saturated vapour pressure and p is the actual gas pressure in the sample cell. Curves a and b denote He gas densities of $n = 5.9 \times 10^{17}$ cm^{-3} and 3.9×10^{17} cm^{-3}, respectively. The maxima at $\Delta\mu/k_B = 7$ K correspond to monolayer completion, the small peaks at 6 K are assigned to the solidification of the first He layer

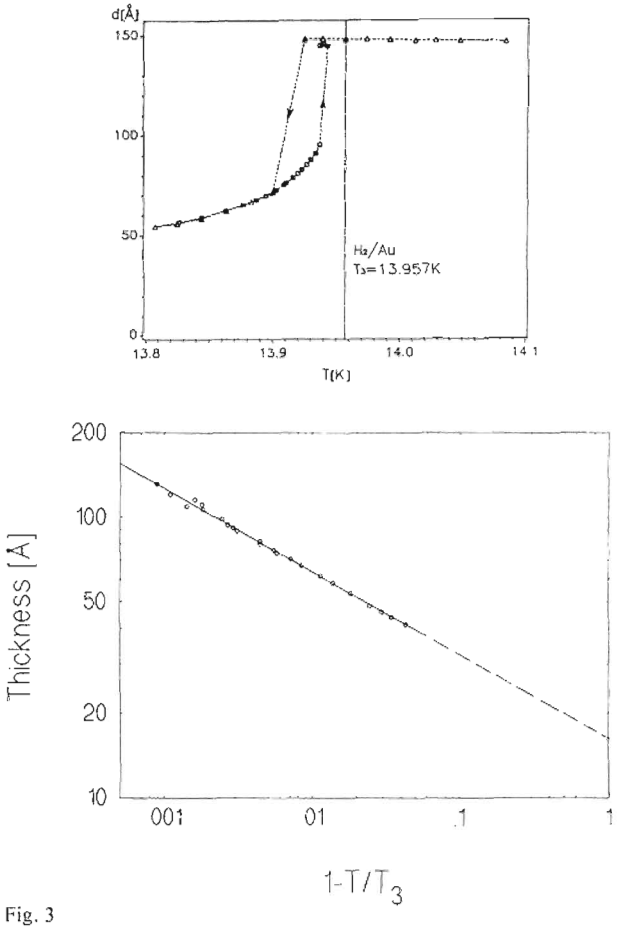

Fig. 3
a) Film thickness d_s of a saturated H_2 film on gold vs. temperature in the vicinity of the triple temperature T_3. The triangles were taken on cooling, the squares on heating. The arrows mark the direction of the jump in d_s; b) Film thickness d_s of the low temperature branch of Fig. 3a plotted vs. the reduced temperature t. The dashed line represents a dependence $d_s \sim t^{-1/3}$

The temperature dependence of d_s shown in Fig. 3a is a clear signature of a transition from incomplete to complete wetting near T_3. In order to work out more explicitly the critical behavior suggested by the increase in thickness on approaching T_3 from below, we have plotted in Fig. 3b the variation of d_s vs. the reduced temperature $t = (T_3 - T)/T_3$ for the low temperature branch. (In these measurements the film was at a slightly higher temperature than the bulk phase. This correction, estimated to 8 mK, is taken into account here). The data can apparently be represented quite well by a power law

$$d_s \sim t^{-a} \tag{1}$$

with $a = (3.00 \pm 0.04)^{-1}$, which is exactly the value expected for systems with van der Waals interaction, found similarly also for other adsorbate-substrate combinations. The fact that d_s remains finite at a value of 150 Å above T_3, instead of diverging as predicted for complete wetting, can be assigned to the small temperature offset from bulk coexistence mentioned above.

Although the power law dependence in Eq. (1) suggests that the transition observed here is a continuous one, the hysteric behavior of the jumps in d_s is at variance with this idea. In fact, the discontinuities could be a signature of prewetting, as it is also observed in the case of He films on weakly binding substrates [3].

III. Quench-condensed Films

According to the data presented in the previous section the maximum equilibrium thickness of H_2 films far below T_3 should only be a few monolayers. On the other hand, arbitrarily thick films can be grown by quench-condensing hydrogen gas onto a sufficiently cold substrate [13]. Since the disordered films formed in this way are in a metastable state, they will undergo an annealing process and change their structure when they are heated to such temperatures that transport by diffusion becomes possible. In Fig. 4 we show the typical annealing behavior of such a quench-condensed hydrogen film, prepared at 1.5 K to an initial thickness of 125 Å, again measured by surface plasmon (SP) resonance and, in addition, by means of light scattering arising from the decay of SP.

Below about 2.8 K all the signals are constant as a function of temperature and show no sign of anncaling effects in the film. Between 2.8 and 3 K, however, there is a strong increase both in the plasmon width and the scattered light intensity (Figs. 4b, c), accompanied by a drastic shift of the apparent film thickness d_{app} to less than half its initial value (Fig. 4a). Both the SP width and the scattered light intensity are a measure of the film roughness on the scale of the light wavelength, which obviously increases sharply in this temperature interval. Upon further heating the signals are again essentially constant, until eventually desorption sets in quite rapidly around 3.6 K, so that the film thickness drops close to zero and also the SP width and scattered light intensity approach their starting values.

The same characteristic behavior with a transition to an intermediate state, though less pronounced, is found also for films with a thickness of only a few monolayers. It is similarly observed for films of the hydrogen isotopes HD and D_2; the transition occurs there around 3.7 and 4.3 K, respectively.

We interpret the observed signals during annealing as being caused by a rearrangement of the molecules in the film, such that crystallites with sizes on the order of the light wavelength form and large portions of the silver substrate are left with a coverage of only a very thin H_2 film, corresponding to the equilibrium thickness under the incomplete wetting conditions at these low temperatures [13]. In addition to the increase in film roughness this gives rise to a drop of the apparent film thickness, because part of the crystallites extend beyond the penetration depth of the SP field and are therefore not "seen" by this probe. Since bulk diffusion so far below the triple point temperature should be negligible, diffusion at the surface appears as the only possible mechanism for such a large-scale rearrangement of hydrogen molecules. From our data we infer that surface

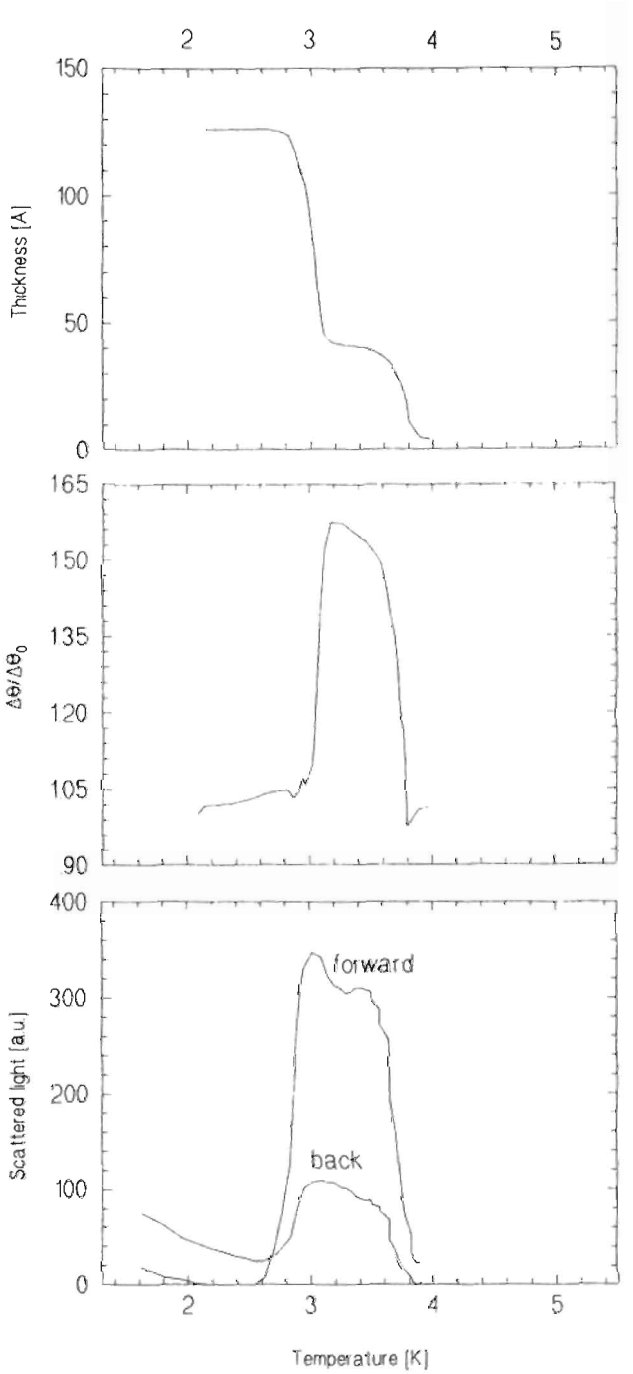

Fig. 4
Annealing behavior of a quench-condensed H_2 film, measured as the film is warmed up at a rate of 1 K/h. a) Apparent thickness (determined from the position of the SP resonance); b) surface plasmon width $\Delta\Theta$, normalized to the width $\Delta\Theta_0$ of the bare silver substrate; c) scattered light intensity at 2 scattering vectors, $3.7\times10^4\,cm^{-1}$ (forward) and $19.5\times10^4\,cm^{-1}$ (back)

diffusion is thermally activated in this case, with an activation energy of about 20 K. Apparently quantum diffusion, which might also come to mind for a system like hydrogen, is not important in the temperature range studied here; it ought to play a role, though, at lower temperatures.

IV. Surface Instabilities

When a bulk system is quenched into a state where it undergoes phase separation, the two limiting mechanisms which describe the initial stage of the separation process are spinodal decomposition and nucleation. The development of a film of initially homogeneous thickness, which becomes unstable due to a change in the wetting conditions or to the onset of diffusion, as just discussed, can in principle proceed along similar routes. As a related macroscopic example of a surface instability we describe here pattern formation at (bulk) helium interfaces, which turns out to be closely analogous to the concepts of spinodal decomposition, with fluctuations on a characteristic length scale growing spontaneously as a result of unstable modes in the system.

We start with the dispersion relation of excitations at the free liquid surface, given by

$$\omega_0^2 = g k + \alpha k^3/\rho \tag{2}$$

where ω_0 and k are the frequency and the wave vector of the surface wave, g is the acceleration due to gravity, α the surface tension and ρ the density of the liquid. Damping is neglected here for simplicity. (The same relation holds, in a slightly modified way, for melting-freezing waves at the liquid-solid interface [15]). When the conditions are changed by charging the surface with electrons, an additional contribution has to be taken into account which *reduces* the frequency of the excitations [16]:

$$\omega^2 = \omega_0^2 - \frac{E_l^2 + E_u^2}{4\pi\rho} k^2 \ . \tag{3}$$

E_l and E_u are the electric fields below and above the surface (related to the surface charge density σ by $E_l - E_u = 2\pi\sigma$). The physical origin for the reduction in ω is that a local elongation of the surface leads to a redistribution of charges and consequently to a nonuniform electrostatic force which counteracts the restoring forces due to gravity and interfacial tension.

According to Eq. (3) one can distinguish two regimes, depending on the control parameter $(E_l^2 + E_u^2)$ [17]: i) As long as this quantity is *below* a critical value ω is still real. Thus the surface remains stable, although softening of the surface excitation spectrum is observed, which is most pronounced at a critical wave vector $k_c = (\alpha/\rho g)^{1/2}$ equal to the inverse capillary length [16]; ii) *above* the critical value of the control parameter the rhs of Eq. (3) becomes negative in a certain range of k vectors around k_c, yielding unstable solutions for the excitations in this region. Consequently the surface starts to deform spontaneously and corrugations at a characteristic wave vector develop. In a small regime just above the instability threshold the deformations may be stabilized by nonlinearities not included in Eq. (3), and a regular array of "dimples" with a lattice constant close to $2\pi k_c^{-1}$ appears (Fig. 5a). Further above the threshold the surface deformations become more irregular, are no longer

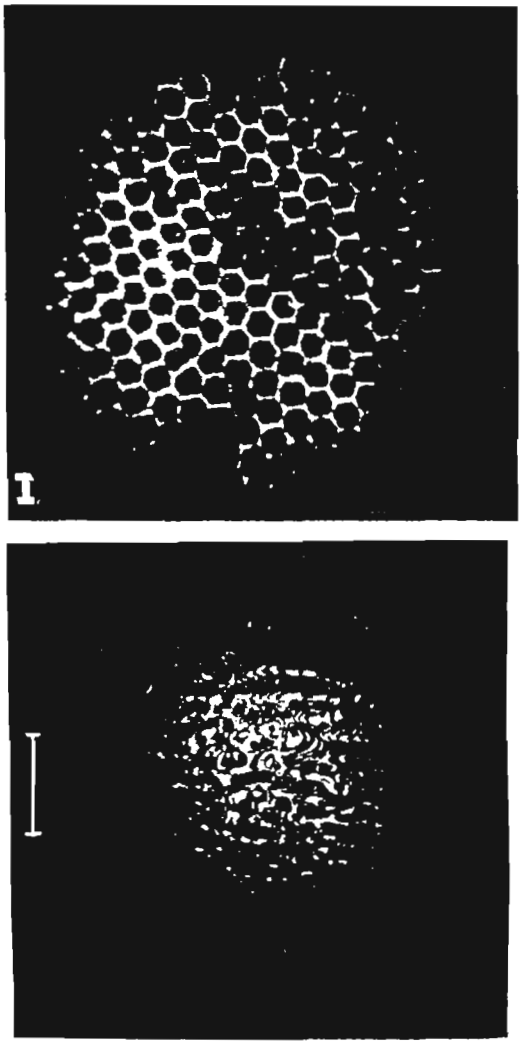

Fig. 5
a) Dimple lattice formed on a charged liquid ^{4}He surface *just above* the critical electric field [17]. Bright contours correspond to local maxima of the He surface. The distance between adjacent rows of dimples is close to the wavelength of the soft ripplon, $2\pi/k_c = 2.4$ mm (indicated by the scale bar); b) snapshot of an electrohydrodynamic instability pattern *well above* threshold ($E/E_c = 2.6$). The system was in this case a charged hcp-superfluid ^{4}He interface. The characteristic distance of the stripes is now distinctly smaller than the wavelength of the soft ripplon (which for this interface is $2\pi/k_c = 6.3$ mm, again marked by the length of the scale bar)

stabilized, and their characteristic length scale decreases (Fig. 5b). The latter behavior is very similar to spinodal decomposition, where the wave vector corresponding to the fastest growth of unstable fluctuations is the larger the deeper the quench.

The electrohydrodynamic instability described here is just one case of a surface instability which develops when an external perturbation is applied to a system with an interface. Another, possibly more general example is the so-called Grinfeld instability which was predicted [18] to occur at a crystal-melt interface when the crystal is subject to uniaxial strain. Like for the electrohydrodynamic instability, corrugations were expected to develop at a wave vector equal to the inverse capillary length. In a recent experiment – once again with a helium interface, in this case between crystal and superfluid phase – the existence of this instability could indeed be demonstrated [19].

The results presented here have been obtained in close collaboration with U. Albrecht, D. Cieslikowski, R. Conradt, W. Ebner, S. Herminghaus, and F. Mugele. Support by the Deutsche Forschungsgemeinschaft, SFB 306, and by the Federal Ministry for Research and Technology (BMFT) is gratefully acknowledged.

References

[1] See, e.g., H. Wiechert, in "Excitations in Two-Dimensional and Three-Dimensional Quantum Fluids", p. 499, eds. A.G.F. Wyatt and H.J. Lauter, Plenum 1991; H.J. Lauter, H. Godfrin, and P. Leiderer, J. Low Temp. Phys. *87*, 425 (1992).
[2] S. Balibar et al., Physica B *169*, 209 (1991) and references therein.
[3] P. Taborek, Discussion Meeting "Phase Transitions at Interfaces" (Bad Herrenalb 1993, this volume); P. Taborek and J.E. Rutledge, Phys. Rev. Lett. *71*, 263 (1993).
[4] H.J. Lauter, H.P. Schildberg, H. Godfrin, H. Wiechert, and R. Haensel, Can. J. Phys. *65*, 1435 (1987).
[5] H.J. Lauter, H. Godfrin, V.L.P. Frank, and P. Leiderer, Phys. Rev. Lett. *68*, 2484 (1992).
[6] D. Cieslikowski, A.J. Dahm, and P. Leiderer, Phys. Rev. Lett. *58*, 1751 (1987).
[7] E. Cheng, M.W. Cole, W.F. Saam, and J. Treiner, Phys. Rev. B *46*, 13967 (1992).
[8] G. Zimmerli, G. Mistura, and M.W.H. Chan, Phys. Rev. Lett. *68*, 60 (1992).
[9] M.A. Paalanen and Y. Iye, Phys. Rev. Lett. *55*, 1761 (1985).
[10] J.G. Brisson, J.C. Mester, and I.F. Silvera, Phys. Rev. B *44*, 12453 (1991).
[11] E. Cheng, G. Ihm, and M.W. Cole, J. Low Temp. Phys. *74*, 519 (1989).
[12] F. Mugele, Diploma Thesis (University of Konstanz, 1993).
[13] P. Leiderer and U. Albrecht, J. Low Temp. Phys. *89*, 229 (1992).
[14] A.D. Migone, A. Hofmann, J.G. Dash, and O.E. Vilches, Phys. Rev. B *37*, 5440 (1988).
[15] K.O. Keshishev, A.Ya. Parshin, and A.V. Babkin, Sov. Phys. JETP *53*, 362 (1981).
[16] P. Leiderer and M. Wanner, Phys. Rev. Lett. *42*, 315 (1979).
[17] P. Leiderer, J. Low Temp. Phys. *87*, 247 (1992).
[18] M.A. Grinfeld, Sov. Phys. Dokl. *31*, 831 (1986).
[19] M. Thiel, A. Willibald, P. Evers, A. Levchenko, P. Leiderer, and S. Balibar, Europhys. Lett. *20*, 707 (1992).

Presented at the Discussion Meeting of the Deutsche Bunsen-Gesellschaft für Physikalische Chemie "Phase Transitions at Interfaces" in Bad Herrenalb, September 22nd to 24th, 1993

E 8530